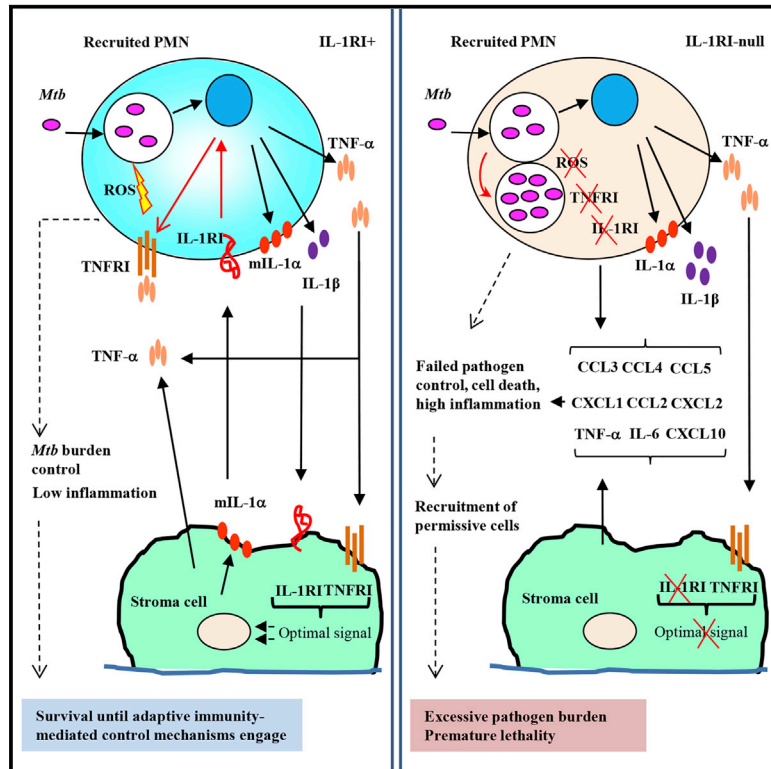


Immunity

Interdependence between Interleukin-1 and Tumor Necrosis Factor Regulates TNF-Dependent Control of *Mycobacterium tuberculosis* Infection

Graphical Abstract



Authors

Nelson C. Di Paolo, Shahin Shafiani, Tracey Day, ..., David Sherman, Kevin Urdahl, Dmitry M. Shayakhmetov

Correspondence

ncdipaolo@emory.edu (N.C.D.P.),
dmitryshay@emory.edu (D.M.S.)

In Brief

IL-1-dependent mechanisms of host resistance to Mtb are not well understood. Shayakhmetov and colleagues demonstrate interdependence between IL-1 and TNF signaling pathways in establishing optimal Mtb control, which operates independently of adaptive immunity. The findings might have implications for refining therapeutic approaches to the disease.

Highlights

- TNF- α fails to control Mtb replication in the absence of functional IL-1RI
- IL-1 and TNF signaling pathways cooperate to establish optimal Mtb control
- IL-1 α is critical for protective granuloma formation
- IL-1 α plays a non-redundant role in mounting host resistance to Mtb



Interdependence between Interleukin-1 and Tumor Necrosis Factor Regulates TNF-Dependent Control of *Mycobacterium tuberculosis* Infection

Nelson C. Di Paolo,^{1,8,*} Shahin Shafiani,^{2,8} Tracey Day,^{2,9} Thalia Papayannopoulou,³ David W. Russell,³ Yoichiro Iwakura,⁴ David Sherman,² Kevin Urdahl,^{2,5} and Dmitry M. Shayakhmetov^{1,6,7,*}

¹Lowance Center for Human Immunology, Emory University, Atlanta, GA 30322, USA

²Center for Infectious Disease Research (formerly Seattle Biomedical Research Institute), Seattle, WA 98109, USA

³Division of Hematology, Department of Medicine, University of Washington, Seattle, WA 98195, USA

⁴Laboratory of Molecular Pathogenesis, Center for Experimental Medicine and Systems Biology, The Institute of Medical Science, The University of Tokyo, Tokyo 108-8639, Japan

⁵Department of Immunology, University of Washington, Seattle, WA 98195, USA

⁶Center for Transplantation and Immuno-mediated Disorders, Emory University, Atlanta, GA 30322, USA

⁷Emory Vaccine Center and Departments of Pediatrics and Medicine, Emory University, Atlanta, GA 30322, USA

⁸Co-first author

⁹Present address: HIV Vaccine Trials Network, Fred Hutchinson Cancer Research Center, Seattle, WA 98109, USA

*Correspondence: ncdipaolo@emory.edu (N.C.D.P.), dmitryshay@emory.edu (D.M.S.)

<http://dx.doi.org/10.1016/j.immuni.2015.11.016>

SUMMARY

The interleukin-1 receptor I (IL-1RI) is critical for host resistance to *Mycobacterium tuberculosis* (Mtb), yet the mechanisms of IL-1RI-mediated pathogen control remain unclear. Here, we show that without IL-1RI, Mtb-infected newly recruited Ly6G^{hi} myeloid cells failed to upregulate tumor necrosis factor receptor I (TNF-RI) and to produce reactive oxygen species, resulting in compromised pathogen control. Furthermore, simultaneous ablation of IL-1RI and TNF-RI signaling on either stroma or hematopoietic cells led to early lethality, indicating non-redundant and synergistic roles of IL-1 and TNF in mediating macrophage-stroma cross-talk that was critical for optimal control of Mtb infection. Finally, we show that even in the presence of functional Mtb-specific adaptive immunity, the lack of IL-1 α and not IL-1 β led to an exuberant intracellular pathogen replication and progressive non-resolving inflammation. Our study reveals functional interdependence between IL-1 and TNF in enabling Mtb control mechanisms that are critical for host survival.

INTRODUCTION

Mycobacterium tuberculosis (Mtb) is one of the leading causes of human mortality associated with a single infection agent worldwide. The stereotypic tissue response to infection with Mtb is the formation of granulomas, a focal inflammatory response where cell-cell cross-talk coordinates cell movement, retention, and function of the granuloma structure (Ramakrishnan, 2012). Previous studies have identified a number of factors and cell subsets of the innate and adaptive immune systems that are crit-

ical for host resistance to Mtb (Cooper, 2009; O'Garra et al., 2013; Ramakrishnan, 2012). It has been demonstrated that mice individually deficient in tumor necrosis factor (TNF) or tumor necrosis factor-receptor I (TNF-RI) (Flynn et al., 1995) are extremely susceptible to low-dose aerosol Mtb infection due to the fundamental role of TNF-RI signaling in maintaining granuloma structure and enabling cell-intrinsic mechanisms of Mtb control (Cantini et al., 2015; Clay et al., 2008; Diedrich et al., 2013). It has also been demonstrated that mice deficient in interleukin-1 α and IL-1 β or IL-1RI (Fremont et al., 2007; Yamada et al., 2000) are extremely susceptible to low-dose aerosol Mtb infection. However, it is unclear why TNF, which is abundantly expressed in the lungs of IL-1-deficient mice, fail to control Mtb in the absence of IL-1 signaling.

IL-1 α and IL-1 β are non-homologous protein members of the IL-1 family cytokines with pleiotropic roles in host immunity, inflammation, and homeostasis (Dinarello, 2009; Garlanda et al., 2013). Both IL-1 α and IL-1 β trigger identical biological responses after binding to the IL-1RI (Dinarello, 2011). In the context of Mtb infection, it remains controversial whether IL-1 α or IL-1 β plays redundant or non-redundant roles in mounting optimal pathogen control. For instance, one study demonstrates that in vivo neutralization of IL-1 α , but not IL-1 β , renders mice highly susceptible to Mtb (Guler et al., 2011). In another study, mice deficient in IL-1 β are shown to be as much susceptible to Mtb as IL-1RI-deficient mice and to succumb to infection within 4 weeks (Mayer-Barber et al., 2010). Moreover, it has been also proposed that during Mtb infection, both IL-1 α and IL-1 β might cooperate in establishing host resistance to Mtb (Mayer-Barber et al., 2011).

To evaluate functional interdependence between the TNF and IL-1 pathways and the individual roles of IL-1 α and IL-1 β ligands in the control of Mtb infection, we performed bone marrow cross-transplantations between wild-type mice and mice deficient in proteins of the IL-1, TNF, or both signaling pathways and analyzed resistance and immuno-pathology of these chimeric mice using a low-dose aerosol infection with Mtb. We

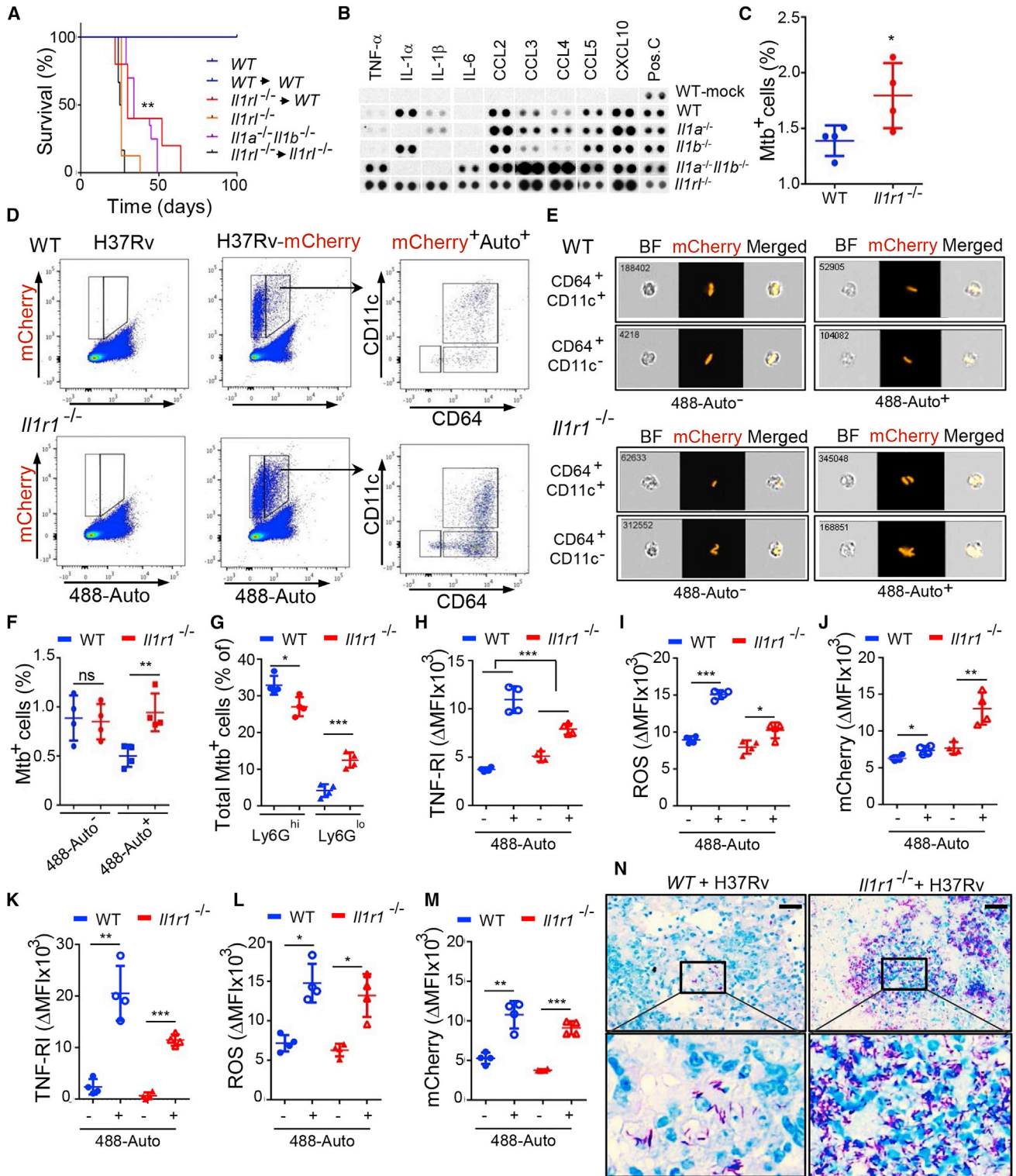


Figure 1. IL-1RI Signaling on Hematopoietic Cells Is Required for Host Resistance to Mtb

(A) Survival of indicated bone marrow chimeric, gene-deficient, and WT mice after infection with Mtb. n = 10 for WT, n = 10 for WT-WT, n = 12 for *Il1r1*^{-/-}-WT, n = 8 for *Il1r1*^{-/-}, n = 6 for *Il1r1*^{-/-}*Il1r1*^{-/-}, and n = 20 for *Il1a*^{-/-}*Il1b*^{-/-} mice. Experimental groups were compared with the log rank test to WT or WT-WT groups. **p < 0.01. (B) Expression of cytokines and chemokines in the lungs of mice deficient for indicated genes or WT mice infected with Mtb 30 days p.i. determined by Proteome Profiler mouse cytokine antibody array. n = 4. Pos-C are dots that show the manufacturer's internal positive control samples on the membrane. WT-mock: the sample of a mouse lung without infection.

(legend continued on next page)

found that IL-1 and TNF play non-redundant and synergistic roles in mediating cross-talk between hematopoietic and stroma cells that is critical for host resistance to Mtb. We further demonstrate that in the presence of functional Mtb-specific adaptive immunity, the lack of IL-1 α and not IL-1 β led to an exuberant intracellular pathogen replication, progressive non-resolving inflammation, and earlier lethality. Together, these data provide mechanistic insights into compartment-specific IL-1RI- and TNF-RI signaling during pulmonary Mtb infection, their functional interdependence for enabling mechanisms of Mtb control, and the critical role of IL-1 α for long-term host survival during Mtb infection.

RESULTS

IL-1RI on Hematopoietic Cells Is Required for Host Resistance to Mtb

Although WT mice or WT mice transplanted with WT bone marrow did not show susceptibility to Mtb infection, *Il1r1*^{-/-} mice, WT mice transplanted with *Il1r1*^{-/-} bone marrow cells, and *Il1r1*^{-/-} mice transplanted with *Il1r1*^{-/-} bone marrow succumbed to Mtb infection, indicating that IL-1RI on hematopoietic cells is critical for host resistance to Mtb (Figure 1A). In agreement with previous reports (Fremont et al., 2007; Mayer-Barber et al., 2011), the analysis of expression of inflammatory cytokines and chemokines 30 days p.i. showed that TNF, IL-6, and key pro-inflammatory chemokines were expressed at much higher amounts in the lungs of Mtb-infected *Il1r1*^{-/-} and *Il1a*^{-/-}*Il1b*^{-/-} mice, when compared to WT, *Il1a*^{-/-}, and *Il1b*^{-/-} mice (Figure 1B), demonstrating that without functional IL-1RI signaling, Mtb infection leads to exuberant inflammation and TNF expression fails to confer protection. In order to understand why IL-1RI-deficient mice succumb to Mtb in the presence of TNF, we next infected WT mice transplanted with bone marrow cells from either WT or *Il1r1*^{-/-} mice with an Mtb strain that expresses the red fluorescent protein mCherry and analyzed expression of TNF-RI and reactive oxygen species (ROS) production in Mtb-infected cells 17 days p.i. This analysis showed that *Il1r1*^{-/-} mice contained higher numbers of Mtb-infected cells in the lungs (Figures 1C and S1A). This gain in Mtb-infected cells in *Il1r1*^{-/-} mice was due to the higher numbers of cells that showed autofluorescence in the 488 channel (488-Auto⁺; Figures 1D–1F and S1B), and more than 95% of these cells express CD64 and CD11b monocytic markers and could be further divided onto distinct CD11c⁺ (myeloid dendritic cells and alveolar macrophages) and CD11c⁻ (newly recruited monocytes, macro-

phages, and PMNs) populations (Figures 1D and S1C; Wolf et al., 2007). Using ImageStream technology, we next confirmed that all cells that appeared mCherry positive by flow cytometry, including those autofluorescent in the 488 channel, were genuinely infected with mCherry-expressing Mtb bacilli (Figure 1E). Because the gain in Mtb-infected cells in *Il1r1*^{-/-} mice, compared to WT mice, was primarily attributable to 488-Auto⁺ CD64⁺CD11c⁻ myeloid cells (Figures 1F and S1B), we next analyzed the cellular composition of this population by using antibodies specific to Ly-6G and CD11b. This analysis showed that this population was composed of Ly6G^{hi}CD11b^{hi} and Ly6G^{lo}CD11b^{lo} cells (PMNs and newly recruited monocytes and macrophages, respectively) (Figure S1C). CD64⁺CD11c⁻Ly6G^{hi} cells represented 33% and 27% of all Mtb-infected cells in WT and *Il1r1*^{-/-} mice, respectively (Figure 1G). In contrast, Mtb-infected CD64⁺CD11c⁻Ly6G^{lo} cells were nearly absent in WT mice and their number was significantly higher in *Il1r1*^{-/-} mice (4% and 12.5%, respectively). The analysis of cell-specific properties of these two populations showed that upon Mtb infection in vivo, the 488-Auto⁻ phenotype associated with uniformly low TNF-RI expression, ROS production, and pathogen burden in both WT and *Il1r1*^{-/-} mice (Figures 1H–1M, 488-Auto⁻ populations). Upon acquisition of 488-Auto⁺ phenotype, in WT mice, CD64⁺CD11c⁻Ly6G^{hi} cells activated high amounts of surface TNF-RI expression and ROS production and exhibited low Mtb burden, indicating effective pathogen control (Figures 1H–1J). In contrast, this population in *Il1r1*^{-/-} mice activated significantly lower amounts of TNF-RI and ROS and failed to control the burden of Mtb at a single-cell level (Figures 1H–1J). The response of CD64⁺CD11c⁻Ly6G^{lo} cells to Mtb infection was qualitatively different and, although activating high amounts of TNF-RI and ROS upon transition to autofluorescent phenotype, this cell population failed to control Mtb burden in both WT and *Il1r1*^{-/-} mice, demonstrating that this cell type, consistent with newly recruited inflammatory monocytes, is intrinsically permissive to Mtb and failed to establish bactericidal state even in WT mice. Importantly, this cell population was only marginally present in WT mice, whereas its proportion was significantly higher in *Il1r1*^{-/-} mice (Figure 1G). Analysis of freshly isolated lung mononuclear cells showed that higher numbers stained positively with necrotic cell dye in *Il1r1*^{-/-} mice, compared to WT mice (Figures S1E and S1F). Furthermore, administration of propidium iodide into Mtb-infected mice revealed extensive distribution of necrotic cells in granulomas of *Il1r1*^{-/-} mice but not in WT mice at 30 days p.i. (Figure S1H). At this time point, the Mtb burden was three orders

(C) Percentage of Mtb-infected mCherry-positive cells in the lungs of WT and *Il1r1*^{-/-} mice 17 days p.i.

(D) Dot plots of cells isolated from the lungs of *Il1r1*^{-/-} and WT mice after infection with H37Rv and mCherry-expressing H37Rv Mtb strains 17 days p.i. with gatings defining autofluorescent and non-autofluorescent populations. The distribution of autofluorescent mCherry⁺ cells on CD11c⁺ and CD64⁺ populations is shown. n = 4.

(E) Images of representative non-autofluorescent (488-Auto⁻) and autofluorescent (488-Auto⁺) cells with indicated markers isolated from the lungs of WT and *Il1r1*^{-/-} mice 17 days p.i., collected with Flow Imager camera.

(F) Percentage of Mtb-infected cells with indicated phenotypes in the lungs of WT and *Il1r1*^{-/-} mice 17 days p.i. n = 4; **p < 0.01.

(G) Percentage of Mtb-infected Ly6G^{hi} and Ly6G^{lo} cell population in the lungs of WT and *Il1r1*^{-/-} mice 17 days p.i. n = 4; *p < 0.05, ***p < 0.001.

(H–J) Expression of TNF-RI (H), ROS (I), and mCherry (J) signal on Mtb-infected 488-Auto⁺ and 488-Auto⁻Ly6G^{hi} cells. n = 4; *p < 0.05, **p < 0.01, ***p < 0.001.

(K–M) Expression of TNF-RI (K), ROS (L), and mCherry (M) signal on Mtb-infected 488-Auto⁺ and 488-Auto⁻Ly6G^{lo} cells. n = 4; *p < 0.05, **p < 0.01, ***p < 0.001.

(N) Macroscopic evaluation of Mtb bacilli distribution on the sections of lungs isolated from WT and *Il1r1*^{-/-} mice 30 days p.i. and stained by acid fast staining. Representative fields are shown. n = 5.

For extended data, see also Figure S1.

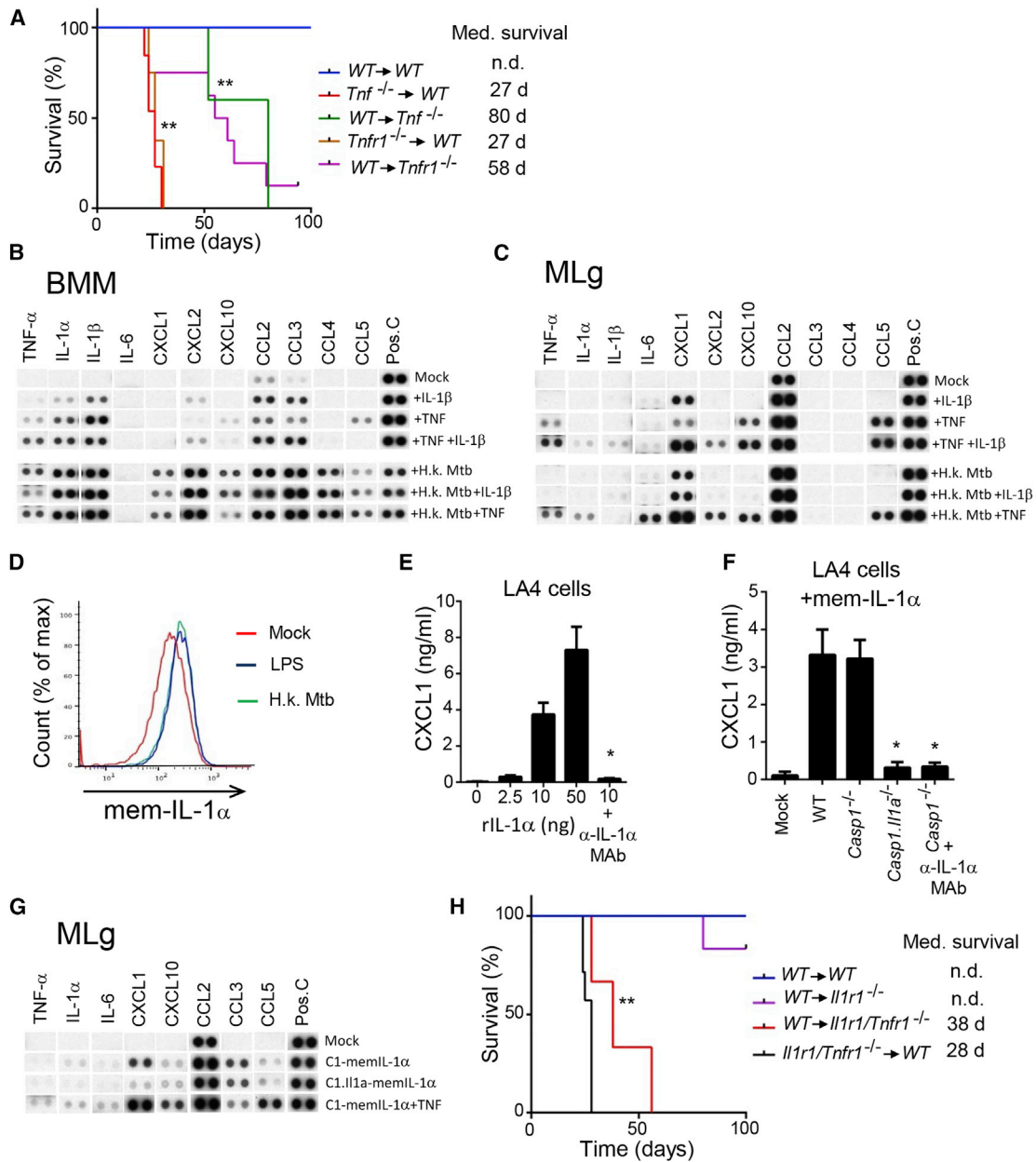


Figure 2. Effective Control of Pulmonary Mtb Infection Is Enabled through IL-1-TNF-Dependent Cytokine-Stroma Cross-talk

(A) Survival of indicated bone marrow chimeric mice after infection with Mtb. n = 5–7 per experimental group. Experimental groups were compared to control WT-WT group with the log rank test. **p < 0.001. Abbreviations are as follows: Med. survival, median survival in days p.i. for groups; n.d., not defined prior to termination of the experiment.

(B and C) Expression of indicated cytokines and chemokines in primary bone marrow macrophages (B) or immortalized mouse lung (MLg) cells (C) after their treatment with IL-1β, TNF, heat-killed Mtb (H.k. Mtb), or their combinations. Cells were analyzed 24 hr after treatment with Proteome Profiler mouse cytokine antibody array. n = 3. Pos-C are dots that show the manufacturer’s internal positive control samples on the membrane. Control cells were treated with media only (Mock).

(D) Expression of IL-1α on the surface of bone marrow macrophages after their treatment with LPS (50 ng/ml) or heat-killed Mtb 4 hr after stimulation and determined by flow cytometry.

(E) Production of CXCL1 chemokine by mouse lung epithelial cell line LA4 after treatment with recombinant mouse IL-1α with or without prior incubation of cells with anti-IL-1α monoclonal Ab (mAb). The amount of CXCL1 was determined by ELISA. n = 4; *p < 0.01.

(F) Production of CXCL1 chemokine by LA4 cells after their co-culture with LPS-treated bone marrow macrophages from WT, *Casp1*^{-/-}, or *Casp1*^{-/-}*Il1a*^{-/-} mice stimulated to produce membrane-bound IL-1α (mem-IL-1α) with or without addition of anti-IL-1α mAb. n = 4; *p < 0.01.

(G) Expression of indicated cytokines and chemokines in MLg cells after their co-culture with LPS-treated bone marrow macrophages from *Casp1*^{-/-} or *Casp1*^{-/-}*Il1a*^{-/-} mice, stimulated to produce membrane-bound IL-1α (C1-memIL-1α or C1.11a-memIL-1α, as a negative control), with or without the addition of TNF. Cells were

(legend continued on next page)

of magnitude higher in *Il1r1*^{-/-} mice, compared to WT mice (Figure S1G), and acid-fast staining of lung sections revealed high numbers of Mtb bacilli localized in cells with interstitial monocyte morphology (Figure 1N).

Together, these data indicate that the lack of IL-1RI on hematopoietic cells results in inability of CD64⁺CD11b⁺CD11c⁻Ly6G^{hi} Mtb-infected cells to upregulate protective amounts of TNF-RI and trigger ROS production, resulting in compromised cell-intrinsic Mtb control. This further associates with the recruitment of Mtb-permissive CD64⁺CD11b⁺CD11c⁻Ly6G^{lo} interstitial monocyte cell pool, exuberant Mtb replication, and early lethality despite abundant TNF expression.

Monocyte-Stroma Cross-talk through IL-1RI and TNF-RI Is Required for Optimal Resistance to Mtb

In order to define the source of IL-1 and TNF and the directionality of host-protective IL-1RI and TNF-RI signaling, we cross-transplanted WT mice with bone marrow from TNF- or TNF-RI-deficient animals. In agreement with earlier studies, mice deficient in TNF or TNF-RI in hematopoietic cells were highly susceptible to Mtb (Figure 2A; Flynn et al., 1995). We further found that *Tnf*^{-/-} and *Tnfr1*^{-/-} mice transplanted with WT bone marrow were also more susceptible to Mtb infection, compared to WT mice transplanted with WT bone marrow, demonstrating that TNF from and TNF-RI on stromal cells were also needed for optimal protection from Mtb (Figure 2A). Treatment of bone-marrow-differentiated macrophages or immortalized mouse lung epithelial (MLg) cells with IL-1β, TNF, and/or heat-killed Mtb (as likely agonists during progressive Mtb infection) showed that combination of IL-1β+TNF or heat-killed Mtb+TNF resulted in the most potent activation of TNF and IL-1α, among other cytokines and chemokines in both cell types (Figures 2B and 2C).

Because IL-1α can function as a membrane-bound cytokine, we treated bone marrow macrophages with LPS or heat-killed Mtb and stained cells with anti-IL-1α Abs. This staining showed that both treatments produced IL-1α-specific staining on non-permeabilized cells (Figure 2D). To analyze whether membrane-IL-1α is biologically active, we exposed reporter cell line LA4 (which produces CXCL1 chemokine in response to recombinant IL-1 [Figure 2E]) to bone marrow macrophages from WT, *Casp1*^{-/-}, or *Casp1*^{-/-}*Il1a*^{-/-} (as negative control) mice treated to produce membrane-bound IL-1α and confirmed that membrane-bound IL-1α on macrophage cells was biologically active and its CXCL1-stimulating activity on LA4 cells could be blocked by anti-IL-1α antibodies (Figure 2F). Moreover, and similar to cell treatment with IL-1β+TNF and heat-killed Mtb+TNF (Figure 2C), MLg cells treated with a combination of TNF and macrophage cells presenting membrane-bound IL-1α led to the most potent activation of cytokines and chemokines when compared to individual treatments (Figure 2G). To ultimately test whether simultaneous IL-1RI and TNF-RI signaling to and from stromal cells is required for host resistance to

Mtb in vivo, we cross-transplanted *Il1r1*^{-/-} or *Il1r1*^{-/-}*Tnfr1*^{-/-} mice with WT bone marrow. Whereas *Il1r1*^{-/-} mice transplanted with WT bone marrow survived up to 100 days p.i. (Figure 2H), WT bone marrow failed to rescue *Il1r1*^{-/-}*Tnfr1*^{-/-} mice, which succumbed to infection with median survival of 38 days. This median survival was significantly lower than that observed in *Tnfr1*^{-/-} mice transplanted with WT bone marrow (58 days), demonstrating that both IL-1RI and TNF-RI signaling on stroma cells are synergistically required for resistance to Mtb.

IL-1α Mediates Host Resistance to Mtb in a Non-redundant Fashion

To define the role of individual IL-1RI ligands during the course of Mtb infection, we infected mice deficient in IL-1RI, IL-1α (Horai et al., 1998), IL-1αβ (Horai et al., 1998), or IL-1β (Shornick et al., 1996) with Mtb. *Il1r1*^{-/-} and *Il1a*^{-/-}*Il1b*^{-/-} mice succumbed to infection with a median survival of 28 and 35 days (Figure 3A). There was a significant divergence in the survival phenotype between *Il1a*^{-/-} and *Il1b*^{-/-} mice, which succumbed to Mtb infection with a median survival of 95 and 152 days p.i., respectively (Figure 3A). These results were reproduced with more virulent Mtb Erdman strain and with highly virulent W-Beijing SA161 strain (Figures S2A and S2B). Bacterial burden analysis in the lungs of WT mice showed a plateau of ~10⁶ CFUs per lung at 30 days p.i., and infection was controlled at this level for more than 200 days. In contrast, *Il1r1*^{-/-} and *Il1a*^{-/-}*Il1b*^{-/-} mice reached a bacterial burden of 10⁸ CFUs by 30 day p.i., and *Il1a*^{-/-} mice reached 10⁸ CFUs by 90 days p.i. (Figure 3B). The Mtb burden in the lungs of *Il1b*^{-/-} and *Casp1*^{-/-}*Casp11*^{-/-} mice was not different from mice in the control group (Figure S2C). Hematoxylin and eosin and acid-fast staining of lung sections revealed that by 60 days p.i. in WT mice, defined granulomas containing few Mtb bacilli were formed. In contrast, lungs in *Il1a*^{-/-} mice contained large inflammatory lesions with highly diffuse structure and cells with numerous bacilli were dispersed throughout the lung parenchyma (Figure 3C). Evaluation of lung histopathology revealed worsening of histopathology score (Figures 3D and S2D) and progressive decline in inflammation-free airway space in the lungs of *Il1a*^{-/-} mice (Figure 3E). Collectively, our analyses show that although within the first 5 weeks p.i. IL-1RI ligands can play compensatory roles in mediating host resistance to Mtb and mice deficient in either IL-1α or IL-1β survive beyond 35 days p.i., IL-1α and IL-1β play non-redundant roles at later times after infection when deficiency in IL-1α compromises host resistance to a significantly greater degree, compared to deficiency in IL-1β.

Mice Deficient in IL-1 Ligands Develop Functional Mtb-Specific Adaptive Immunity

The delayed susceptibility of *Il1a*^{-/-} mice to pulmonary Mtb infection could be explained by a requirement of IL-1α for

analyzed 24 hr after treatment with Proteome Profiler mouse cytokine antibody array. n = 3. Pos-C are dots that show the manufacturer's internal positive control samples on the membrane. Control cells were treated with media only (Mock).

(H) Survival of indicated bone marrow chimeric mice after infection with Mtb. n = 5–7 per experimental group. Experimental groups were compared to control WT-WT group with the log rank test. **p < 0.001. Abbreviations are as in (A).

Error bars represent SEM.

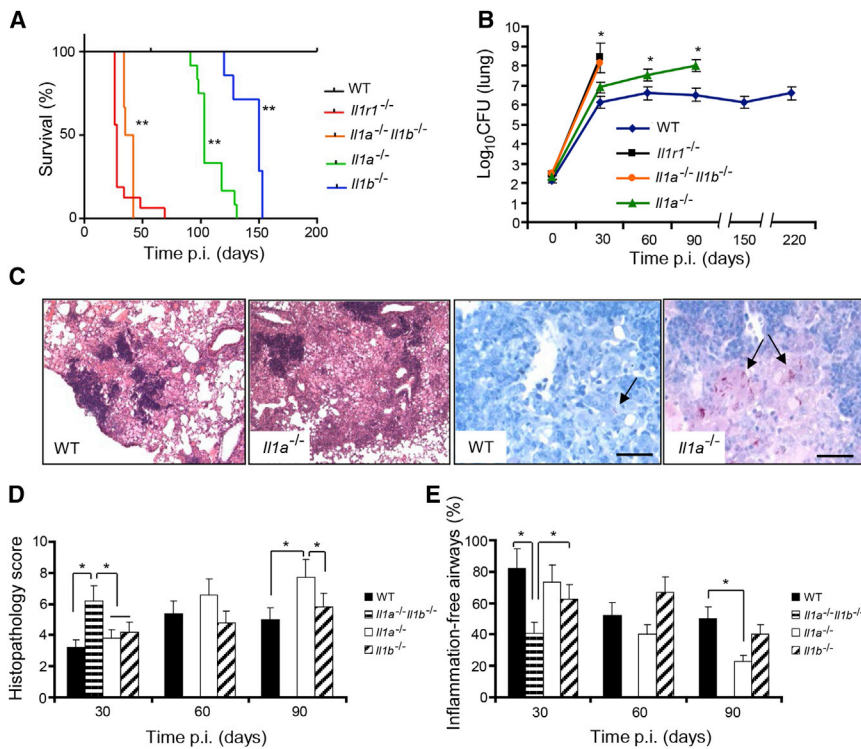


Figure 3. IL-1 α and IL-1 β Play Distinct Roles in Mediating Long-Term Resistance to Mtb

(A) Survival of indicated gene-deficient mice after infection with Mtb. $n = 12$ for WT, $n = 14$ for $Il1r1^{-/-}$, $n = 13$ for $Il1a^{-/-}Il1b^{-/-}$, $n = 12$ for $Il1a^{-/-}$, and $n = 9$ for $Il1b^{-/-}$ mice. $**p < 0.01$.

(B) Bacterial loads in the lungs of Mtb-infected mice as evaluated by plating serial dilutions of lung homogenates on 7H10 agar. Data are representative of three independent experiments with five mice per experimental group per time point. $*p < 0.01$.

(C) Lung histopathology in WT and $Il1a^{-/-}$ at 60 days after infection with Mtb analyzed after hematoxylin and eosin (H&E) staining (left). Right panels show lung sections stained with acid-fast staining with Mtb bacilli indicated by arrows. The representative images after H&E (left) and acid fast (right) staining are shown. Scale bars represent 50 μm .

(D) Quantitative representation of the lung histopathology in WT, $Il1a^{-/-}$, $Il1b^{-/-}$, and $Il1a^{-/-}Il1b^{-/-}$ mice at 30, 60, and 90 days after infection with Mtb analyzed after hematoxylin and eosin (H&E) staining using histopathology score scale shown in Figure S2D. Four consecutive sections of the lungs at three depth levels per each mouse were evaluated. The histopathology score was averaged for five mice per each experimental group per time point. $*p < 0.05$.

(E) Quantitative representation of the inflammation-free airway space in the lungs of WT, $Il1a^{-/-}$, $Il1b^{-/-}$, and $Il1a^{-/-}Il1b^{-/-}$ mice at 30, 60, and 90 days after infection with Mtb analyzed after hematoxylin and eosin (H&E) staining. Four consecutive sections of the lungs at three depth levels per each mouse were evaluated. The data were averaged for five mice per each experimental group per time point. $*p < 0.05$. Error bars represent SEM. For extended data, see also Figure S2.

an effective adaptive immune response (Ben-Sasson et al., 2009). To test this hypothesis, we used MHC class I and II tetramers to track CD8⁺ and CD4⁺ T cells recognizing *Mtb* immunodominant MHC class I (TB10.4₄₋₁₁:K^b) and MHC class II (ESAT-6₄₋₁₇:I-A^b)-restricted T cell responses in the lungs of WT, $Il1a^{-/-}$, and $Il1a^{-/-}Il1b^{-/-}$ mice. At 30 days p.i., this analysis revealed similar frequencies of tetramer-binding CD4⁺ and CD8⁺ T cells in all groups (Figures 4A–4D and S3). To determine the frequency of IFN- γ -producing T cells in vivo, we also performed direct ex vivo intracellular IFN- γ staining on freshly isolated lung lymphocytes in the absence of in vitro stimulation (Shafiani et al., 2010). This analysis revealed significantly higher proportions of IFN- γ -producing cells within the tetramer-binding CD4⁺ and CD8⁺ populations of $Il1a^{-/-}$ and $Il1a^{-/-}Il1b^{-/-}$ mice, compared to control group, at 30 days p.i. (Figures 4B and 4D). The higher frequency of IFN- γ -producing T cells in $Il1a^{-/-}$ and $Il1a^{-/-}Il1b^{-/-}$ mice demonstrate that T cells from these strains are not intrinsically deficient in their ability to express IFN- γ in vivo. In vitro stimulation of lung lymphocytes, freshly isolated from Mtb-infected WT and $Il1a^{-/-}$ mice, with the anti-CD3 and anti-CD28 Abs, ESAT-6₄₋₁₇, or TB10.4₄₋₁₁ peptides did not reveal any differences in the proportions of IFN- γ - or TNF-producing CD4⁺ and CD8⁺ T cells between the groups (Figures 4E and 4F). Therefore, these analyses show that the development of *Mtb*-specific adaptive immunity does not depend on IL-1 cytokines.

The Lack of IL-1 α -IL-1RI Signaling Leads to a Non-protective Highly Inflammatory State and Premature Lethality

Gross examination of the Mtb-infected mice showed that by 90 days p.i., the wet lung weight for $Il1a^{-/-}$ mice exceeded that for WT animals by 180% ($p < 0.01$, Figure 5A) and the number of mononuclear cells harvested from the lungs of $Il1a^{-/-}$ mice was significantly greater than from the WT mice both at 60 and 90 days p.i. ($p < 0.01$, Figure 5B). The frequency of Ly-6G⁺Ly-6C⁺ polymorphonuclear (PMN) leukocyte population at this late time point was lower in $Il1a^{-/-}$ mice (1.88%) compared to WT animals (3.14%, $p < 0.05$, Figure 5C), excluding the possibility that the pulmonary pathology in $Il1a^{-/-}$ mice is associated with neutrophilic inflammation. This analysis also revealed that the majority of leukocytes purified from the lungs of $Il1a^{-/-}$ mice expressed Ly-6C marker, associated with inflammatory monocytes, macrophages, and dendritic cells (DCs) (De Trez et al., 2009; Mayer-Barber et al., 2011; Swirski et al., 2009). To better define the in vivo activation status of monocytes accumulated in the lungs of WT and $Il1a^{-/-}$ mice after Mtb infection, we assessed isolated lung cells for expression of CD11b and CD11c, as well as Ly-6C and CD40 as markers associated with cellular activation. We observed a dramatic increase in Ly-6C expression by both CD11b⁺ and CD11c⁺ cell populations isolated from $Il1a^{-/-}$ mice, compared to WT animals ($p < 0.01$, Figure 5D). In addition, the population of CD11c^{hi}Ly-6C^{int} monocytes observed in WT was absent in $Il1a^{-/-}$ mice (population a,

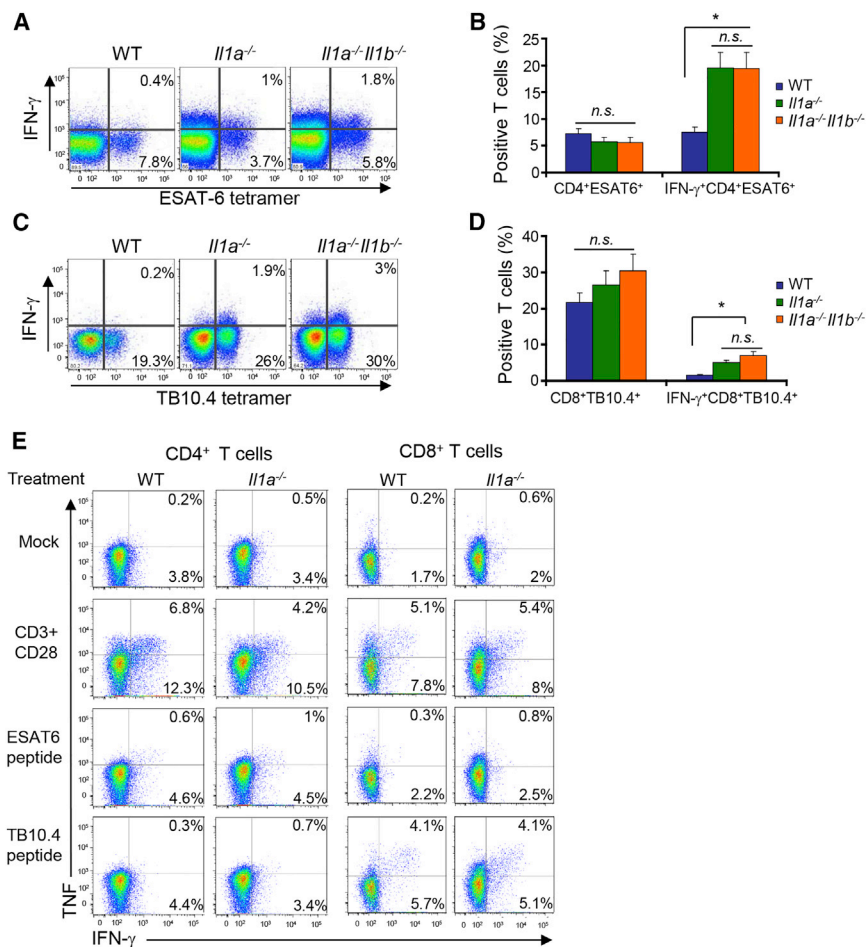


Figure 4. Mice Deficient in IL-1RI Ligands Develop Functional Pathogen-Specific Adaptive Immunity

(A) Representative dot plots showing the proportion of IFN- γ -producing cells in populations of ESAT6₄₋₁₇:I-A^b-specific CD4⁺ T cells purified from the lungs of WT, *Il1a*^{-/-}, and *Il1a*^{-/-}*Il1b*^{-/-} mice at 30 days after Mtb infection. n = 4.

(B) Quantitative representation of data shown in (A). *p < 0.001. Abbreviation is as follows: n.s., not significant.

(C) Representative dot plots showing the proportion of IFN- γ -producing cells in populations of TB10.4*:K^b-specific CD8⁺ T cells purified from the lungs of WT, *Il1a*^{-/-}, and *Il1a*^{-/-}*Il1b*^{-/-} mice at 30 days after Mtb infection. n = 4.

(D) Quantitative representation of data shown in (C). *p < 0.001. Abbreviation as in (B).

(E) Flow cytometry analysis of IFN- γ and TNF expression by CD4⁺ and CD8⁺ T cells purified from the lungs of WT or *Il1a*^{-/-} mice 60 days after infection with Mtb and re-stimulated with indicated stimuli in vitro. Purified cells were stimulated with the media only (Mock), a mixture of anti-CD3 and anti-CD28 antibodies, or synthetic ESAT6 (ESAT-6₄₋₁₇ peptide) or TB10.4 (TB10.4₄₋₁₁ peptide)-specific peptides, respectively. Cumulative data showing the average percentages of lung CD4⁺ or CD8⁺ T cells producing IFN- γ and TNF in response to indicated stimuli in individual mice (three mice per group) are shown. No statistically significant differences in in vitro responses to analyzed stimuli between cells purified from WT and *Il1a*^{-/-} mice were found.

Error bars represent SEM. For extended data, see also Figure S3.

Figure 5D). The analysis of CD40 expression on lung leukocytes showed that after Mtb infection, the proportion of highly activated CD11c^{hi}CD40^{hi} monocytes was more than 2-fold higher in *Il1a*^{-/-} mice compared to WT animals (Figure 5E). Furthermore, a distinct population of CD11c^{hi}CD40^{lo} monocytes that was observed in WT animals was completely missing from the lungs of *Il1a*^{-/-} mice (population b, Figure 5E).

Next, we generated bone marrow chimeras in which lethally irradiated WT mice were transplanted with either WT or *Il1a*^{-/-} bone marrow cells. Five months after hematopoietic reconstitution, chimeric mice were infected with Mtb and Ly-6C and CD40 marker expression on their CD11c⁺ cells were analyzed 90 days p.i. We observed that CD11c⁺ cells in chimeric mice recapitulated the phenotypes observed in mice from which the donor bone marrow cells were derived (Figure 5F). Collectively, these data show that in IL-1 α -deficient mice, the higher inflammatory state does not correlate with improved resistance to Mtb but rather is associated with progressive non-resolving monocytic inflammation that constrains free airway space and leads to premature lethality.

Restoration of IL-1 α Expression in CD11c⁺ Cells of *Il1a*^{-/-} Mice Alleviates Inflammation and Improves Survival after Mtb Infection

To determine whether and what kind of Mtb-infected cells express IL-1 α in the lungs of Mtb-infected mice, we analyzed

sections of lungs from Mtb-infected mice stained with fluorescent IL-1 α -specific antibody and polyclonal Mtb-specific antibody or antibodies for various cellular markers by confocal microscopy (Di Paolo et al., 2009). At 60 days p.i., those cells that stained positive for Mtb antigens also stained positive for IL-1 α (Figure 6A), and IL-1 α -staining co-localized with CD11c⁺ and CD11b⁺ cells but not with CD3⁺ or Gr1⁺ cells (Figure 6B).

Because the majority of lung leukocytes including alveolar macrophages, immature DCs, and activated DCs express CD11c, we next determined whether the restoration of IL-1 α expression specifically in CD11c⁺ cells would suffice to rescue the susceptibility of *Il1a*^{-/-} mice to Mtb infection. We utilized a foamy virus vector-based stable gene transfer approach (Figure S4A; Josephson et al., 2002), where mouse IL-1 α gene was expressed under the control of a minimal *Itgax* promoter (Ni et al., 2009). CD11c^{hi}CD40^{lo} monocyte population was restored in Mtb-infected *Il1a*^{-/-} mice transplanted stem cells transduced with *Itgax*-IL-1 α virus (Figure 6C) but not *Itgax*-stop-IL-1 α virus (Figure 6D). Importantly, the median survival of *Il1a*^{-/-} mice transplanted with *Itgax*-stop-IL-1 α vector-transduced stem cells was only 55 days, whereas 8 out of 9 *Il1a*^{-/-} mice transplanted with hematopoietic stem cells transduced with *Itgax*-IL-1 α virus mice survived beyond 80 days after Mtb infection (p < 0.001, Figure 6E). Therefore, our data show that

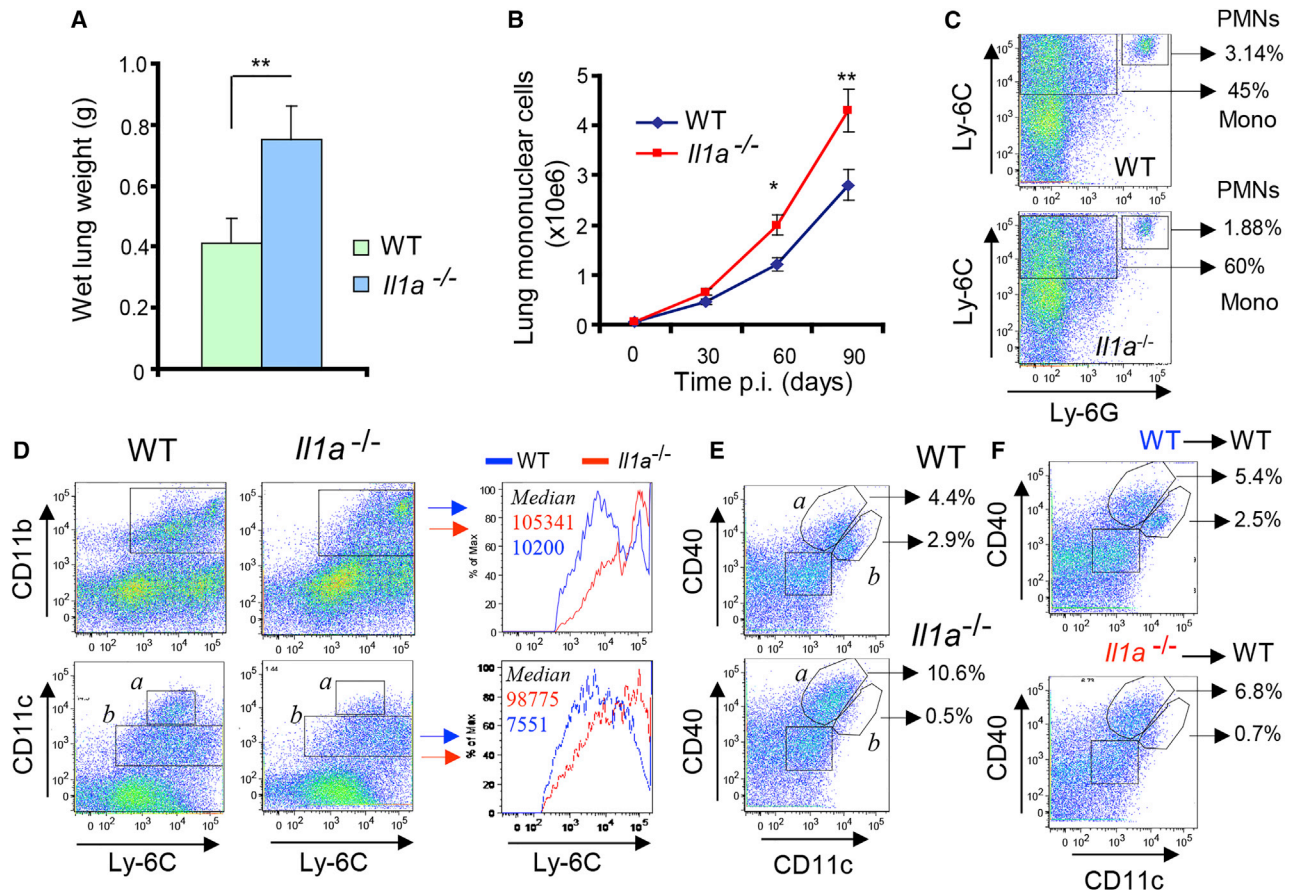


Figure 5. The IL-1 α -Deficient Mice Develop Non-resolving Monocytic Inflammation

(A) The weight of lungs harvested from WT and *Il1a*^{-/-} mice at 90 days after Mtb infection. n = 30; **p < 0.01.

(B) Total number of mononuclear cells purified from lungs of WT and *Il1a*^{-/-} mice at indicated times after Mtb infection. n = 5; *p < 0.05, **p < 0.01.

(C) Flow cytometry dot plots of the distribution of Ly-6C- and Ly-6G-expressing cell subsets in the lungs of WT and *Il1a*^{-/-} mice 90 days after Mtb infection. The average percentage of Ly-6C⁺ or Ly-6C⁺Ly-6G⁺ populations are shown for each strain. n = 4.

(D) Analysis of Ly-6C expression on CD11b- and CD11c-expressing subsets of mononuclear cells purified from the lungs of Mtb-infected WT and *Il1a*^{-/-} mice. Median intensity of Ly-6C staining on CD11b⁺ and CD11c⁺ (population b) subsets are shown in histogram plots on the right. n = 4. a and b designate individual Ly-6C⁺ cell populations expressing different amounts of CD11c.

(E) Analysis of CD40-expressing CD11c⁺ cell subsets in the lungs of WT and *Il1a*^{-/-} mice after Mtb infection. The average percentage of CD11c⁺CD40^{hi} (population a) and CD11c^{hi}CD40^{lo} (population b) subset are shown. n = 4.

(F) Flow cytometry dot plots of CD11c⁺CD40⁺ cells in the lungs of bone marrow chimeric WT mice, transplanted with either WT or *Il1a*^{-/-} bone marrow cells. Recipient WT mice were lethally irradiated and transplanted with bone marrow cells from either WT or *Il1a*^{-/-} mice. Five months after the bone marrow transplantation, mice were infected with Mtb and indicated cell subsets were analyzed in the lungs 80 days after infection. Average percentage of CD11c⁺CD40^{hi} and CD11c^{hi}CD40^{lo} are shown. n = 3.

Error bars represent SEM.

cell-type-specific restoration of IL-1 α expression in CD11c⁺ cells in *Il1a*^{-/-} mice results in lung cell phenotypes comparable to WT mice and prolonged survival after Mtb infection.

IL-1 α Is Required for Intracellular Control of Mtb Replication at a Single-Cell Level In Vivo via Cell-Extrinsic Mechanism

To reveal the mechanism of IL-1 α -mediated control of Mtb resistance, we analyzed the dynamics of Mtb replication in vivo. Quantification of Mtb bacilli on acid-fast-stained sections of lungs revealed that the number of bacilli per high power view field rapidly increased and peaked by 30 days p.i. in all groups (Figure 7A). Of note, although granulomatous areas in the lungs

expanded continuously over time (Figures 3D and 3E), by 60 days p.i., the number of bacilli per view field drastically declined in WT mice and remained low until 100 days p.i., implying the effective control of Mtb. In contrast, the number of bacilli in lung sections was significantly higher for *Il1a*^{-/-} and *Il1a*^{-/-}*Il1b*^{-/-} mice at 30 days p.i., compared to WT animals (Figure 7A), suggesting that these mice were deficient in their ability to control Mtb replication during early infection. Of note, as in WT animals, the number of bacilli per view field in *Il1a*^{-/-} mice declined to a similar degree between days 30 and 60 p.i., but it increased significantly again by 100 days p.i.

Detailed evaluation of lung sections of *Il1a*^{-/-} and WT mice at day 60 p.i. revealed that in *Il1a*^{-/-} mice, more than 80% of

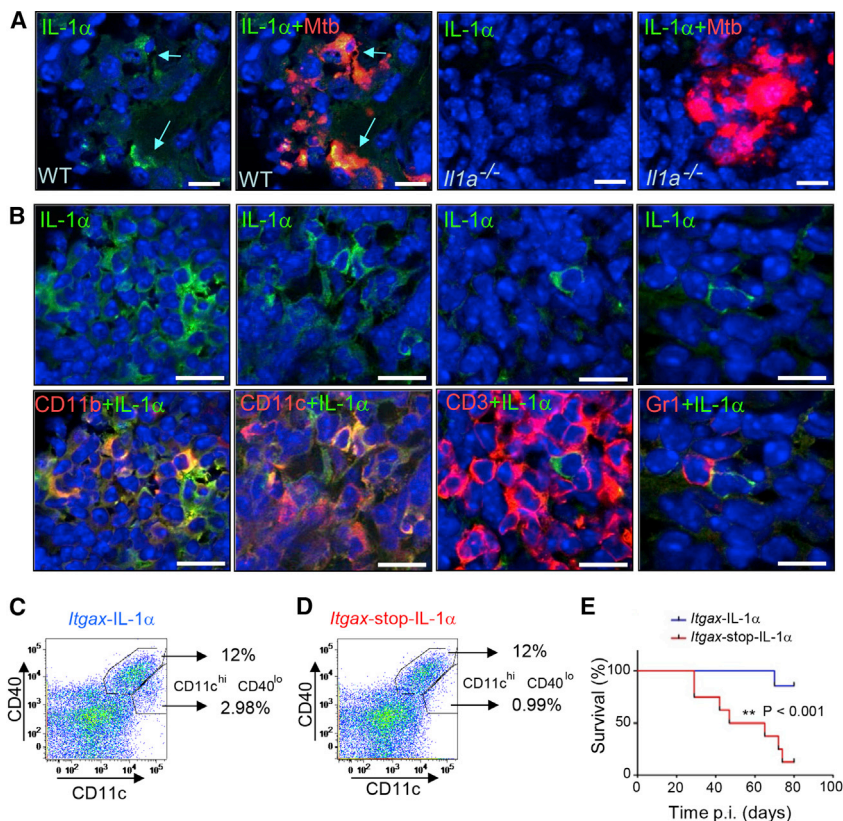


Figure 6. Restoration of IL-1 α Expression in CD11c⁺ Cells Alleviates Pulmonary Mtb Susceptibility Phenotype of IL-1 α -Deficient Mice

(A) Confocal microscopy analysis of IL-1 α expression in Mtb-infected cells of lung granulomas 60 days after infection on frozen OCT-embedded sections of lungs. IL-1 α -specific antibody staining was developed with Cy2-labeled secondary antibody (green). Mtb antigens were stained with polyclonal primary antibody and developed with Cy3-labeled secondary antibody (red). Mtb-infected cells stained positive with IL-1 α antibody are indicated by arrows. Scale bars represent 20 μ m. Confocal images were obtained with a Zeiss 510 Meta Confocal microscope. Representative fields are shown. n = 4.

(B) Confocal microscopy analysis of IL-1 α expression in cells of lung granulomas 60 days after infection on frozen OCT-embedded sections of lungs. IL-1 α -specific antibody staining was developed with Cy2-labeled secondary antibody (green). CD11b, CD11c, CD3, and Gr1 antigens were stained with rat monoclonal primary antibody and developed with Cy3-labeled secondary antibody (red). Scale bars represent 20 μ m. Representative fields are shown. n = 4.

(C and D) Analysis of CD40-expressing CD11c⁺ cell subsets in the lungs of *Il1a*^{-/-} mice transplanted with foamy-virus-infected hematopoietic stem cells 60 days after Mtb infection. The average percentages of CD11c⁺CD40^{hi} and CD11c⁺CD40^{lo} subset are shown. (E) Survival of mice transplanted with CD11c-IL-1 α - or CD11c-stop-IL-1 α -foamy virus-transduced hematopoietic stem cells after their infection with Mtb. n = 10 for each experimental group. **p < 0.001. Groups were compared with a log rank test.

For extended data, see also Figure S4.

individual Mtb-infected cells contained more than four bacilli per cell, whereas in WT animals, only 45% of infected cells contained more than four bacilli (Figures 7B and 7C). Furthermore, electron microscopy analysis showed that Mtb bacilli in *Il1a*^{-/-} mice could be found in clusters (Figures 7D and S5), suggesting bacterial replication in vivo. Using a previously described “Mtb replication clock” approach to quantify the rate of Mtb replication in vivo (Gill et al., 2009), we calculated Mtb replication rates in *Il1a*^{-/-} and WT mice. Between days 1 and 11 p.i., the Mtb population in the lungs of *Il1a*^{-/-} mice replicated at a rate of 0.77 per day, corresponding to a 31.17 hr generation time. In contrast, Mtb population in the lungs of WT mice replicated at a significantly slower rate of 0.55 per day, corresponding to 43.64 hr generation time (p < 0.01, Figure 7E).

We hypothesized that if the defect in Mtb replication control in *Il1a*^{-/-} mice is entirely cell intrinsic, it should be possible to be reproduced in vitro. We differentiated macrophages from the bone marrow of WT or *Il1a*^{-/-} mice, infected them with Mtb, and analyzed the bacterial burden over time. We also treated Mtb-infected cells with IL-1 α , IFN- γ , or a combination of both to determine whether these cells were deficient in restricting Mtb replication even in the presence of these exogenous cytokines. We found that Mtb replicated equally efficiently in both WT and *Il1a*^{-/-} macrophages. Furthermore, in agreement with an earlier study, IFN- γ was highly effective at restricting Mtb replication in vitro (MacMicking et al., 2003), and WT and *Il1a*^{-/-} macrophages were equally responsive to IFN- γ and exhibited

reduced Mtb CFUs (Figures S5B and S5C). The addition of IL-1 α to Mtb-infected cells did not restrict bacterial growth. Taken together, these data show that *Il1a*^{-/-} mice fail to control Mtb replication at a single-cell level and this inability to control Mtb replication is not cell intrinsic.

DISCUSSION

In this study we have analyzed the functional role of the compartment-specific IL-1RI and TNF-RI signaling and the individual contribution of IL-1-RI ligands in mediating host resistance to pulmonary Mtb infection in mice. Numerous previous studies demonstrated that TNF and/or TNF-RI expression in hematopoietic cells is absolutely required for the host resistance to Mtb. Indeed, WT mice transplanted with bone marrow from *Tnf*^{-/-} or *Tnfr1*^{-/-} mice were shown to be extremely susceptible to Mtb infection and succumb in 4 weeks. We report here that TNF from and TNF-RI on stromal cells are also required to mediate optimal host resistance to Mtb. Although TNF-RI signaling is pivotal for protective immunity against Mtb (Flynn et al., 1995), abundant TNF expression in the lungs of IL-1RI-deficient mice fails to provide protection and *Il1r1*^{-/-} mice also succumb to Mtb infection within 4 weeks (Fremont et al., 2007; Sugawara et al., 2001). Collectively, these results obtained with mice deficient in individual components of distinct molecular pathways indicate that these cytokines cannot fully compensate for the lack of one another, thus highlighting their

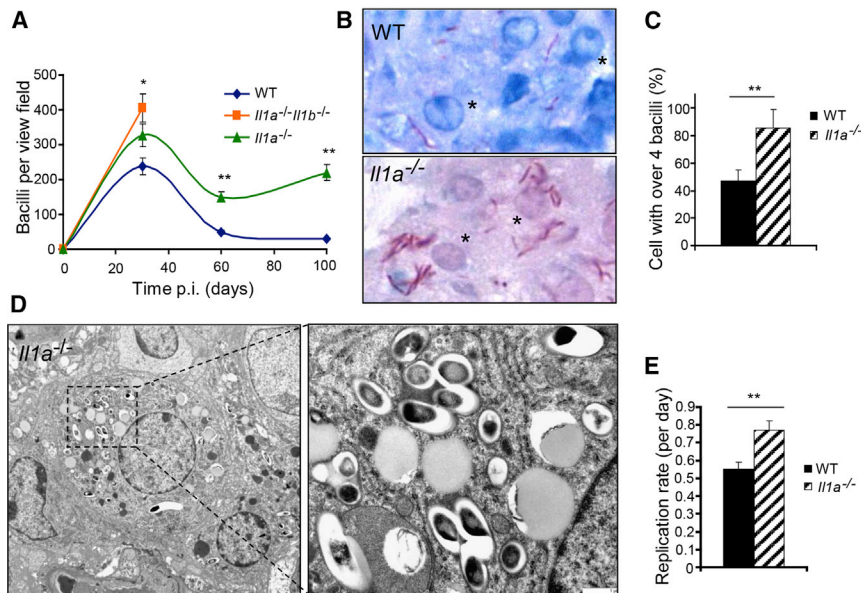


Figure 7. IL-1 α Is Required for Intracellular Control of Mtb Replication In Vivo

(A) The number of Mtb bacilli on acid fast-stained sections of mouse lungs at indicated time point. The numbers of bacilli were counted for seven view fields at four tissue depth levels per mouse and were averaged for five mice per experimental group per time point. * $p < 0.05$, ** $p < 0.01$.

(B) Representative fields of granulomas with Mtb-infected cells (depicted with stars) in the lungs of WT and *Il1a^{-/-}* mice at 60 days p.i. Lung sections were stained with acid fast to visualize Mtb bacilli (pink). (C) Quantitation of cells containing fewer than or more than four Mtb bacilli on the sections of lungs from WT or *Il1a^{-/-}* mice 60 days p.i. Cells were quantified on lung sections as described in (A).

(D) Electron microscopy analysis of cells infected with Mtb in the lungs of *Il1a^{-/-}* mice 60 days p.i. Left: original magnification 5,000 \times ; right: selected area of an infected cell at magnification of 30,000 \times . Representative cell is shown. $n > 50$.

(E) Mtb replication rate between days 1 and 11 in the lungs of WT and *Il1a^{-/-}* mice determined based on pBP10 plasmid frequency and previously described mathematical model (Gill et al., 2009). ** $p < 0.01$.

Error bars represent SEM. For extended data and the model, see also Figures S5 and S6.

non-redundant and synergistic roles in mounting effective protection from Mtb.

It was recently proposed that the mechanism of IL-1-dependent control of Mtb is related to COX2-dependent synthesis of prostaglandin E2 (PGE2), which, in turn, suppresses IFN-I, which has pro-pathogenic properties (Mayer-Barber et al., 2014). However, earlier studies on leukocyte dynamics in the lungs of mice at early time points after Mtb infection show that the likely pro-pathogenic function of IFN-I depends on its ability to recruit Mtb-susceptible monocyte subsets to the lungs (Desvignes et al., 2012). Furthermore, *Ilnar1^{-/-}* mice had lower pathogen burden in the lungs 18 days p.i. and demonstrated no difference in bacterial burden at 24 days p.i. compared to WT mice (Desvignes et al., 2012). These data suggest that IFN-I signaling is likely to be dispensable for early cell-intrinsic pathogen control and unlikely to be relevant to mechanisms allowing for exacerbated replication of Mtb in the lungs of *Il1r1^{-/-}* mice that succumb by 4 weeks p.i.

Here we found that IL-1 and TNF signaling to and from the hematopoietic and stromal compartments cooperated to control early Mtb infection. When hematopoietic cells lacked IL-1RI signaling, the mice were severely susceptible to Mtb infection and the presence of TNF could not compensate for this deficiency. Our data show that when IL-1RI is completely lacking, a population of bona fide neutrophils with CD11b⁺CD11c⁻Ly6G^{hi} markers in Mtb-infected mice fail to upregulate TNF-RI and produce ROS, leading to significantly higher bacterial burden and higher necrotic death in vivo, thus suggesting that this specific population of cells might require IL-1RI-dependent licensing to upregulate TNF-RI and induce ROS production in vivo. The excessive Mtb replication and necrotic death led to hyperinflammation and the recruitment to the lungs of CD64⁺CD11b⁺Ly6G^{lo} monocytes, which were highly permissive to

Mtb irrespective of high amounts of TNF-RI or ROS production. The population of highly Mtb-permissive CCR2⁺ monocytes as propagators of mycobacterial infection has been recently described and is consistent with our findings (Cambier et al., 2014; Lyadova et al., 2010). We further found that the exposure of immortalized mouse lung epithelial cells to a combination of IL-1 β and TNF or heat-killed Mtb and TNF resulted in a robust up-regulation of TNF and IL-1 α expression in these non-hematopoietic cells. It is noteworthy that although the lack of either TNF-RI or IL-1RI on stromal cells allowed for relatively long survival of mice, the lack of both of these receptors simultaneously on stromal cells resulted in the collapse of host resistance despite the presence of both receptors on WT hematopoietic cells. Taken together, these data provide direct evidence for non-redundant and synergistic roles of IL-1RI- and TNF-RI-dependent signaling in mediating cross-talk between stroma and hematopoietic cells that is necessary for the optimal control of Mtb infection.

Our study also revealed that IL-1 α , a key cytokine implicated in driving host responses to cell damage and sterile inflammation (Chen et al., 2007), plays a critical and non-redundant role in host protection against pulmonary Mtb in a non-cell-intrinsic manner. The *Il1a^{-/-}* mice succumb consistently earlier than *Il1b^{-/-}* mice upon infection with Mtb strains of different virulence. Although TNF signaling was earlier implicated in maintaining *M. marinum* granuloma structure in zebrafish model, TNF signaling is not required for granuloma formation (Clay et al., 2008). During chronic Mtb infection of *Il1a^{-/-}* mice, we observed large diffuse inflammatory lesions and dispersed distribution of Mtb-infected cells, suggesting an important role of IL-1 α -driven cell-cell cross-talk for coordinating protective granuloma formation or maintenance. IL-1 α can function as a plasma membrane-bound cytokine (Dinarello, 2009; Huleihel et al., 1990; Kurt-Jones et al., 1985; Niki et al., 2004). Because granuloma formation is

principally a focal inflammatory response to Mtb infection, the key role of IL-1 α in driving cell-cell cross-talk might be an essential function of this cytokine to ensure host protection and pathogen control. In this context, although our study provides direct evidence that IL-1 α -deficient mice failed to control Mtb replication at the level of individual infected cells, this defect manifests itself only in vivo and is not cell intrinsic. Indeed, Mtb bacilli replicated in vitro with identical efficacy in bone-marrow-derived macrophages harvested from either WT or *Il1a*^{-/-} mice. Our findings comparing *Il1a*^{-/-} and *Il1b*^{-/-} mice seem to contradict previously reported data, which demonstrate that IL-1 β -deficient mice are highly susceptible to Mtb and died within 4 weeks p.i., similar to IL-1RI-deficient mice (Mayer-Barber et al., 2010). In our study and the study reported by Mayer-Barber, the specific inactivating mutations of *Il1b* are distinct (Horai et al., 1998; Shornick et al., 1996) and might explain the discrepancy between our findings.

Clearly, understanding the mechanistic role of IL-1- and TNF-driven cell-cell crosstalk in triggering innate mechanisms of host resistance to Mtb can provide the rationale for the development of approaches and drugs to limit the incidence of both progressive and latent tuberculosis through modulating pathways of innate immunity.

EXPERIMENTAL PROCEDURES

Experimental Animals

All studies were conducted in accordance with the National Institutes of Health Guide for the Care and Use of Laboratory Animals and the Institutional Animal Care and Use Committee guidelines of the University of Washington and Seattle Biomedical Research Institute where all the work involving animals was conducted. C57BL/6 mice were purchased from Charles River. *Il1r1*^{-/-} and *Tnf*^{-/-} mice were purchased from Jackson Laboratory. *Casp1*^{-/-} *Casp11*^{-/-} mice were kindly provided by Dr. R. Flavell (Yale University) and described in Kuida et al. (1995), and *Il1a*^{-/-} and *Il1a*^{-/-} *Il1b*^{-/-} mice were described in Horai et al. (1998). *Il1b*^{-/-} mice were described in Shornick et al. (1996). All mice were on C57BL/6 genetic background, matched by age, and housed in specific-pathogen-free facilities.

Bacterial Infection

Stock of Mtb strains H37Rv, H37Rv::pBP10 (Gill et al., 2009), Erdman, or W-Beijing SA161 were sonicated before use, and mice were infected in an aerosol infection chamber (Glas-Col). To determine the Mtb burden, at indicated times the left lung of each mouse was homogenized in PBS with 0.05% Tween 80. 10-fold serial dilutions were made in PBS with 0.05% Tween 80 and plated on Mitchison 7H10 plates. Colonies were counted after 21 days of incubation at 37°C, and CFUs per organ were determined. Approximately 100 CFUs were deposited in the lungs of each mouse upon initial infection. Mice were sacrificed when the body weight declined by 20%, compared to the body weight of each animal at the day of infection.

Histology and Immunofluorescence Staining

For hematoxylin and eosin, acid-fast Kinyoun's, and electron microscopy studies, the right lung was excised, fixed in 4% paraformaldehyde (PFA) for 1 week at room temperature, embedded in paraffin, and sectioned by microtome in consecutive sections of 5 μ m. For confocal immunofluorescence, staining was performed on frozen sections. For PI analyses, dry frozen sections were evaluated under a fluorescent microscope without further processing.

Cell Isolation, Staining, and Flow Cytometry

In brief, single-cell suspensions of intraparenchymal lung lymphocytes were stained at saturating conditions using antibodies specific for CD3 (145-2C11), CD4 (RM4-5), CD8 (53-6.7), CD11c (HL), CD11b (M1/70), Gr-1 (RB6-8C5), CD45.2 (104), CD45.1 (A20), Ly-6C (HK1.4), Ly-6G (1A8), or CD40 (1C10), all from BD Biosciences. IFN- γ and TNF intracellular staining was per-

formed using a kit as instructed by the manufacturer (BD), with minor modifications. For direct ex vivo detection of IFN- γ , lung cells were isolated in the presence of Brefeldin A (Sigma) and staining for surface markers and intracellular IFN- γ was performed as described, without in vitro restimulation. A minimum of 100,000 live cells per sample was acquired on an LSRII instrument with the FACSDiva software (BD Biosciences). The samples were then analyzed by Flowjo Software (Tree Star). TNF-RI and mCherry analyses were done using CD64 and CD11c-gating approach (Figure S1A). ROS staining was analyzed using alternate CD11b and CD11c-gating approach (Figure S1D) to avoid spectral overlap between ROX reagent and CD64 Ab staining.

Detection of ESAT-6₄₋₁₇- and TB10.4₄₋₁₁-Specific Cells

PE-labeled MHC class II tetramers (I-A^b) containing the stimulatory residues 4 to 17 (QQWNFAGIEAAASA) of the early secreted antigenic target 6 kD (ESAT-6) of Mtb and APC-labeled MHC class I tetramers (K^b) containing the stimulatory residues 4 to 11 (IMYNYPAM) of the low-molecular-weight protein antigen TB10.4 of Mtb (obtained from the NIH Tetramer Core Facility) were used to detect Mtb-specific CD4⁺ and CD8⁺ T cells, respectively.

Statistical Analysis

All experiments were repeated at least twice and a minimum number of samples analyzed per each experimental group was equal to three or more. Results are expressed as mean and standard error. Unless otherwise indicated, Student's unpaired two-tailed t test was used for comparing experimental groups, with $p < 0.05$ considered significant.

SUPPLEMENTAL INFORMATION

Supplemental Information includes six figures and Supplemental Experimental Procedures and can be found with this article online at <http://dx.doi.org/10.1016/j.immuni.2015.11.016>.

AUTHOR CONTRIBUTIONS

N.C.D.P. and D.M.S. conceived the study, N.C.D.P. and S.S. conducted most of the experiments, T.D. performed experiments and analyzed plasmid-based Mtb replication in vivo, T.P. and D.W.R. provided advice on and shared reagents for bone marrow transplantation studies and foamy virus production, Y.I., D.S., and K.U. shared critical reagents, K.U., N.C.D.P., and D.M.S. guided the study and analyzed the data, and N.C.D.P. and D.M.S. wrote the manuscript. All authors discussed the results and commented on the manuscript.

ACKNOWLEDGMENTS

We are thankful to Alan Aderem (Center for Infectious Disease Research) for providing *Casp1*^{-/-} *Casp11*^{-/-} and *Il1b*^{-/-} mice from colonies at the Institute for Systems Biology (Seattle, WA). We are grateful to John MacMicking (Yale University School of Medicine), James Sisson (Center for Infectious Disease Research), and Ron N. Apte (Ben-Gurion University of the Negev) for helpful discussion. We thank Raymond Kong, Robert Thacker, and Amnis-EMD Millipore for generously sharing their expertise and facilities to run Image-Stream analyses. We thank Stephanie Larra (University of Washington) for technical assistance with electron microscopy analyses. This study was supported by the Grand Challenges Explorations grant from the Bill and Melinda Gates Foundation #51778; NIH grants AI065429 and AI107960, and Children's Healthcare of Atlanta (CHOA) Research Trust support to D.M.S.; and by NIH U19 AI106761 and AI076327 and the Paul G. Allen Family Foundation grants to K.U.

Received: August 19, 2013

Revised: May 4, 2015

Accepted: November 19, 2015

Published: December 15, 2015

REFERENCES

Ben-Sasson, S.Z., Hu-Li, J., Quiel, J., Cauchetaux, S., Ratner, M., Shapira, I., Dinarello, C.A., and Paul, W.E. (2009). IL-1 acts directly on CD4 T cells to

- enhance their antigen-driven expansion and differentiation. *Proc. Natl. Acad. Sci. USA* **106**, 7119–7124.
- Cambier, C.J., Takaki, K.K., Larson, R.P., Hernandez, R.E., Tobin, D.M., Urdahl, K.B., Cosma, C.L., and Ramakrishnan, L. (2014). Mycobacteria manipulate macrophage recruitment through coordinated use of membrane lipids. *Nature* **505**, 218–222.
- Cantini, F., Nannini, C., Niccoli, L., Iannone, F., Delogu, G., Garlaschi, G., Sanduzzi, A., Maticchi, A., Prignano, F., Conversano, M., and Goletti, D.; SAFEBIO (Italian multidisciplinary task force for screening of tuberculosis before and during biologic therapy) (2015). Guidance for the management of patients with latent tuberculosis infection requiring biologic therapy in rheumatology and dermatology clinical practice. *Autoimmun. Rev.* **14**, 503–509.
- Chen, C.J., Kono, H., Golenbock, D., Reed, G., Akira, S., and Rock, K.L. (2007). Identification of a key pathway required for the sterile inflammatory response triggered by dying cells. *Nat. Med.* **13**, 851–856.
- Clay, H., Volkman, H.E., and Ramakrishnan, L. (2008). Tumor necrosis factor signaling mediates resistance to mycobacteria by inhibiting bacterial growth and macrophage death. *Immunity* **29**, 283–294.
- Cooper, A.M. (2009). Cell-mediated immune responses in tuberculosis. *Annu. Rev. Immunol.* **27**, 393–422.
- De Trez, C., Magez, S., Akira, S., Ryffel, B., Carlier, Y., and Muraille, E. (2009). iNOS-producing inflammatory dendritic cells constitute the major infected cell type during the chronic *Leishmania major* infection phase of C57BL/6 resistant mice. *PLoS Pathog.* **5**, e1000494.
- Desvignes, L., Wolf, A.J., and Ernst, J.D. (2012). Dynamic roles of type I and type II IFNs in early infection with *Mycobacterium tuberculosis*. *J. Immunol.* **188**, 6205–6215.
- Di Paolo, N.C., Miao, E.A., Iwakura, Y., Murali-Krishna, K., Aderem, A., Flavell, R.A., Papayannopoulou, T., and Shayakhmetov, D.M. (2009). Virus binding to a plasma membrane receptor triggers interleukin-1 alpha-mediated proinflammatory macrophage response in vivo. *Immunity* **31**, 110–121.
- Diedrich, C.R., Mattila, J.T., and Flynn, J.L. (2013). Monocyte-derived IL-5 reduces TNF production by *Mycobacterium tuberculosis*-specific CD4 T cells during SIV/M. tuberculosis coinfection. *J. Immunol.* **190**, 6320–6328.
- Dinarello, C.A. (2009). Immunological and inflammatory functions of the interleukin-1 family. *Annu. Rev. Immunol.* **27**, 519–550.
- Dinarello, C.A. (2011). Interleukin-1 in the pathogenesis and treatment of inflammatory diseases. *Blood* **117**, 3720–3732.
- Flynn, J.L., Goldstein, M.M., Chan, J., Triebold, K.J., Pfeffer, K., Lowenstein, C.J., Schreiber, R., Mak, T.W., and Bloom, B.R. (1995). Tumor necrosis factor-alpha is required in the protective immune response against *Mycobacterium tuberculosis* in mice. *Immunity* **2**, 561–572.
- Fremont, C.M., Togbe, D., Doz, E., Rose, S., Vasseur, V., Maillet, I., Jacobs, M., Ryffel, B., and Quesniaux, V.F.J. (2007). IL-1 receptor-mediated signal is an essential component of MyD88-dependent innate response to *Mycobacterium tuberculosis* infection. *J. Immunol.* **179**, 1178–1189.
- Garlanda, C., Dinarello, C.A., and Mantovani, A. (2013). The interleukin-1 family: back to the future. *Immunity* **39**, 1003–1018.
- Gill, W.P., Harik, N.S., Whiddon, M.R., Liao, R.P., Mittler, J.E., and Sherman, D.R. (2009). A replication clock for *Mycobacterium tuberculosis*. *Nat. Med.* **15**, 211–214.
- Guler, R., Parihar, S.P., Spohn, G., Johansen, P., Brombacher, F., and Bachmann, M.F. (2011). Blocking IL-1 α but not IL-1 β increases susceptibility to chronic *Mycobacterium tuberculosis* infection in mice. *Vaccine* **29**, 1339–1346.
- Horai, R., Asano, M., Sudo, K., Kanuka, H., Suzuki, M., Nishihara, M., Takahashi, M., and Iwakura, Y. (1998). Production of mice deficient in genes for interleukin (IL)-1alpha, IL-1beta, IL-1alpha/beta, and IL-1 receptor antagonist shows that IL-1beta is crucial in turpentine-induced fever development and glucocorticoid secretion. *J. Exp. Med.* **187**, 1463–1475.
- Huleihel, M., Douvdevani, A., Segal, S., and Apte, R.N. (1990). Regulation of interleukin 1 generation in immune-activated fibroblasts. *Eur. J. Immunol.* **20**, 731–738.
- Josephson, N.C., Vassilopoulos, G., Trobridge, G.D., Priestley, G.V., Wood, B.L., Papayannopoulou, T., and Russell, D.W. (2002). Transduction of human NOD/SCID-repopulating cells with both lymphoid and myeloid potential by foamy virus vectors. *Proc. Natl. Acad. Sci. USA* **99**, 8295–8300.
- Kuida, K., Lippke, J.A., Ku, G., Harding, M.W., Livingston, D.J., Su, M.S.S., and Flavell, R.A. (1995). Altered cytokine export and apoptosis in mice deficient in interleukin-1 beta converting enzyme. *Science* **267**, 2000–2003.
- Kurt-Jones, E.A., Beller, D.J., Mizel, S.B., and Unanue, E.R. (1985). Identification of a membrane-associated interleukin 1 in macrophages. *Proc. Natl. Acad. Sci. USA* **82**, 1204–1208.
- Lyadova, I.V., Tsiganov, E.N., Kapina, M.A., Shepelkova, G.S., Sosunov, V.V., Radaeva, T.V., Majorov, K.B., Shmitova, N.S., van den Ham, H.J., Ganusov, V.V., et al. (2010). In mice, tuberculosis progression is associated with intensive inflammatory response and the accumulation of Gr-1 cells in the lungs. *PLoS ONE* **5**, e10469.
- MacMicking, J.D., Taylor, G.A., and McKinney, J.D. (2003). Immune control of tuberculosis by IFN-gamma-inducible LRG-47. *Science* **302**, 654–659.
- Mayer-Barber, K.D., Barber, D.L., Shenderov, K., White, S.D., Wilson, M.S., Cheever, A., Kugler, D., Hieny, S., Caspar, P., Núñez, G., et al. (2010). Caspase-1 independent IL-1beta production is critical for host resistance to mycobacterium tuberculosis and does not require TLR signaling in vivo. *J. Immunol.* **184**, 3326–3330.
- Mayer-Barber, K.D., Andrade, B.B., Barber, D.L., Hieny, S., Feng, C.G., Caspar, P., Oland, S., Gordon, S., and Sher, A. (2011). Innate and adaptive interferons suppress IL-1 α and IL-1 β production by distinct pulmonary myeloid subsets during *Mycobacterium tuberculosis* infection. *Immunity* **35**, 1023–1034.
- Mayer-Barber, K.D., Andrade, B.B., Oland, S.D., Amaral, E.P., Barber, D.L., Gonzales, J., Derrick, S.C., Shi, R., Kumar, N.P., Wei, W., et al. (2014). Host-directed therapy of tuberculosis based on interleukin-1 and type I interferon crosstalk. *Nature* **511**, 99–103.
- Ni, J., Nolte, B., Arnold, A., Fournier, P., and Schirmacher, V. (2009). Targeting anti-tumor DNA vaccines to dendritic cells via a short CD11c promoter sequence. *Vaccine* **27**, 5480–5487.
- Niki, Y., Yamada, H., Kikuchi, T., Toyama, Y., Matsumoto, H., Fujikawa, K., and Tada, N. (2004). Membrane-associated IL-1 contributes to chronic synovitis and cartilage destruction in human IL-1 alpha transgenic mice. *J. Immunol.* **172**, 577–584.
- O'Garra, A., Redford, P.S., McNab, F.W., Bloom, C.I., Wilkinson, R.J., and Berry, M.P. (2013). The immune response in tuberculosis. *Annu. Rev. Immunol.* **31**, 475–527.
- Ramakrishnan, L. (2012). Revisiting the role of the granuloma in tuberculosis. *Nat. Rev. Immunol.* **12**, 352–366.
- Shafiani, S., Tucker-Heard, G., Kariyone, A., Takatsu, K., and Urdahl, K.B. (2010). Pathogen-specific regulatory T cells delay the arrival of effector T cells in the lung during early tuberculosis. *J. Exp. Med.* **207**, 1409–1420.
- Shornick, L.P., De Togni, P., Mariathasan, S., Goellner, J., Strauss-Schoenberger, J., Karr, R.W., Ferguson, T.A., and Chaplin, D.D. (1996). Mice deficient in IL-1beta manifest impaired contact hypersensitivity to trinitrochlorobenzene. *J. Exp. Med.* **183**, 1427–1436.
- Sugawara, I., Yamada, H., Hua, S., and Mizuno, S. (2001). Role of interleukin (IL)-1 type 1 receptor in mycobacterial infection. *Microbiol. Immunol.* **45**, 743–750.
- Swirski, F.K., Nahrendorf, M., Etzrodt, M., Wildgruber, M., Cortez-Retamozo, V., Panizzi, P., Figueiredo, J.L., Kohler, R.H., Chudnovskiy, A., Waterman, P., et al. (2009). Identification of splenic reservoir monocytes and their deployment to inflammatory sites. *Science* **325**, 612–616.
- Wolf, A.J., Linas, B., Trevejo-Núñez, G.J., Kincaid, E., Tamura, T., Takatsu, K., and Ernst, J.D. (2007). *Mycobacterium tuberculosis* infects dendritic cells with high frequency and impairs their function in vivo. *J. Immunol.* **179**, 2509–2519.
- Yamada, H., Mizuno, S., Horai, R., Iwakura, Y., and Sugawara, I. (2000). Protective role of interleukin-1 in mycobacterial infection in IL-1 alpha/beta double-knockout mice. *Lab. Invest.* **80**, 759–767.